Journal of Theoretical and Applied Mechanics, Sofia, Vol.54 (2024) pp. 391-404
SPECIAL ISSUE

OPTIMAL VERSUS SUBOPTIMAL TUNED MASS DAMPERS: A COMPARISON STUDY BASED ON ENERGY TRANSFER BETWEEN PRIMARY AND SECONDARY SYSTEMS

GEORGIOS I. DADOULIS, GEORGE D. MANOLIS*, KONSTANTINOS V. KATAKALOS

Laboratory of Experimental Strength of Materials and Structures, Department of Civil Engineering, Aristotle University, Thessaloniki, GR-54124, Greece

[Received: 30 September 2024. Accepted: 14 December 2024]

doi: https://doi.org/10.55787/jtams.24.54.4.391

ABSTRACT: The passage of heavy traffic in bridges potentially causes damage, which can be limited by passive device configurations such as the widely used tuned mass damper (TMD). In here, we investigate the vibratory motion caused by a heavy mass sliding on a simply supported bridge deck with a TMD attached at center span. The TMD, modelled as a single-degree-of-freedom (SDOF) secondary system comprising a mass and spring, is attached to the bottom flange to act as an energy absorber of vibrations coming from the primary system (the bridge). This sub-optimal TMD without a damper is analyzed using a Lagrangian energy balance formulation to derive the governing equations of motion, followed by a time-stepping numerical solution. Results are given in terms of time histories and power spectral densities, which allows for an investigation of the transmission of vibratory energy between primary and secondary systems. These numerical simulations help gauge the performance of a number of TMD configurations with optimized material parameters, using as benchmark the sub-optimal TMD where damping is provided by the spring element only.

KEY WORDS: Tuned mass dampers; beams; moving loads; energy transfer; vibrations

1 INTRODUCTION

Tuned mass damper (TMD) technology has its origins in the early 1900's [1] and is characterized by mechanical simplicity, cost effectiveness and reliability. The two basic fields of application are civil engineering [2] for motion control (bridges, towers, tall buildings) and mechanical engineering for vibration suppression in turbines and various types of machines [3]. Early studies in optimized TMD design for harmonic

*Corresponding author e-mail: gdm@civil.auth.gr

motions can be traced to Ref. [4] and the random excitations to Ref. [5]. In principle, TMD's can completely absorb vibrations at a selected frequency band, while material damping in the primary structure to which they are attached also plays a significant role in this respect, as it increases the frequency bandwidth of the response in the vicinity of the tuned frequency.

Standard TMD design [6] is basically an SDOF dynamic system comprising a spring plus a damper connected to a small mass. Thus, we have a secondary system attached to a primary system, i.e., to the structure itself. In terms of analysis, the latter may be represented as either a multi-degree-of-freedom (MDOF) system or as a continuous system. In either case, TMD's operate very close to the dominant mode of vibration of the primary structure, resulting in a substantial reduction of its dynamic responses. However, this vibration minimization is also dependent on the frequency content of the external loads, which implies that optimization is required in order for the TMD to operate in the most sensitive frequency band. Alternatively, nonlinear TMD's may be designed [7] which exhibit a variable (i.e., load dependent) natural frequency. A classification [8] of basic TMD technology distinguishes between (i) composite TMD design, (ii) distributed TMD design, (iii) MDOF TMD design and (iv) impact dampers in conjunction with a TMD. In terms of recent applications, we mention the numerical investigation of the performance of a TMD in controlling the torsional vortex phenomenon for an aerodynamically streamlined twin-box girder suspension bridge [9]. The TMD parameters were gauged in terms of controlling the torsional response of the suspension bridge, and an effective range was reached and compared with the output provided by a genetic algorithm. Recent work on the use of TMD's for vibration suppression includes Ref. [10] on the performance of a suspension bridge under the combined effect of wind and traffic, Ref. [11] on use of the theory of generalized functions to formulate and solve the equations of motion for a viscoelastic Bernoulli –Euler beam with rotational joints and multiple supports under a moving force, Ref. [12] on the installation of two TMD's in a footbridge for pedestrian use, and finally Ref. [13] on the coupled bridge-moving vehicle system with the possibility of using the latter component as a TMD. It is noted in passing that the vibratory energy in the TMD can theoretically be harvested [7] for local use such to power a local monitoring system or for lighting the bridge.

In this work, we investigate the transfer of vibratory energy between a bridge and an attached TMD as a heavy mass moves across its span, see Fig. 1. The motivation for this work stems from earlier field measurements by the authors [14] on the vibrations of overpasses due to vehicular traffic and of pedestrian bridges due to pedestrian traffic. Specifically, the bridge is a simply supported girder and the point mass slides across the span with constant velocity. What makes the problem challenging is that that the travelling mass magnitude is comparable to that of the bridge span, ranging

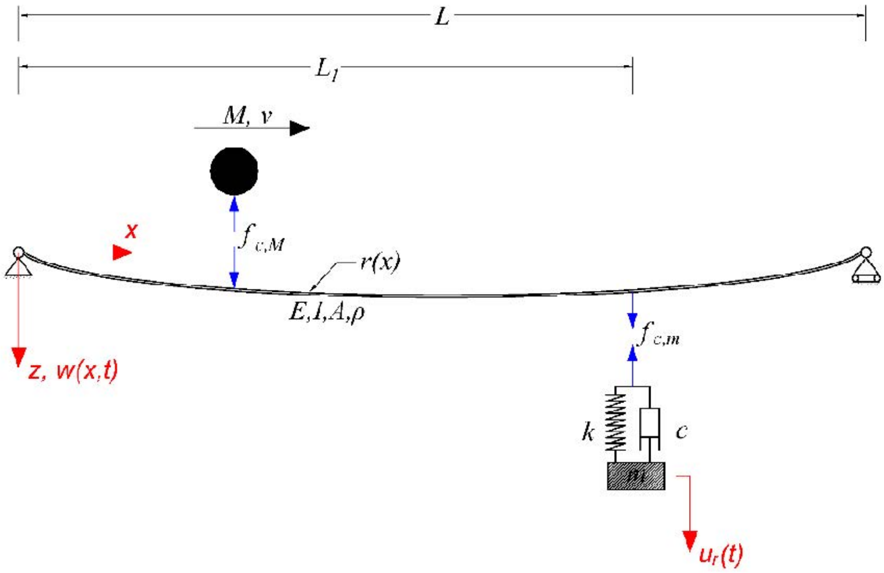

Fig. 1. Simply supported bridge deck with an attached TMD under a moving heavy mass.

from 15% up to 40%, which results in an eigenvalue problem is time-dependent during the traverse time, indicating a non-conservative system [15]. The TMD is kept as simple as possible, comprising a mass and a spring with minimal damping provided by the spring itself. As shown in Fig. 2, energy is transferred between all three components of the coupled structural system, namely the travelling mass (the forcing

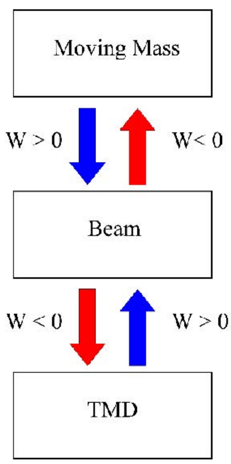

Fig. 2. Energy transfer within the moving mass-bridge deck-TMD coupled system.

function), the bridge deck (the primary system) and the TMD (the secondary system). The design philosophy is to have the TMD passively absorb energy from the bridge deck so as to minimize its dynamic response.

2 Mathematical Model

The solution of the coupled primary-secondary system [16] yields the kinematic field that develops because of the moving mass in terms of the bridge displacement generalized coordinates and the TMD vertical displacement as $\mathbf{q}^{\mathrm{T}}(t) = [q_1\,(t)\,q_2\,(t)\,u_r\,(t)]$. Transforming the generalized coordinates into the physical coordinates, i.e., the transverse displacements of the bridge, we have that $w\,(x,t) = \Phi_i\,(x)\,q_i\,(t)$ where $\Phi_i(x)$ are the eigenfunctions of the beam. As the mass M slides along the deck with constant velocity v, the transverse displacement at any point on the bridge and that at the TMD location $x = L_1$ are respectively given as follows:

$$w\,(vt,t) = \Phi_i\,(vt)\,q_i\,(t)\,, \qquad w\,(L_1,t) = \Phi_i\,(L_1)\,q_i\,(t) + u_r\,(t)\,. \tag{1}$$

Next, in reference to the vibratory energy which develops in the coupled system, the general expression for work W done by all forces present in the dynamic system are

$$W = \int\limits_c \vec{F}d\vec{r}, \qquad \vec{F} = (PQR),\, d\vec{r} = (dxdydz) \tag{2}$$

with c the path followed by the general force $\vec{F}$. More specifically, P, Q, R respectively are the force vector components including the contact forces f_c that develop at location L_1. Expanding Eq. (2) and considering only the work done in the vertical direction gives

$$W = \int\limits_c Pdx + Qdy + Rdz \Longrightarrow W = \int\limits_c Rdz = \int\limits_0^t R(dz/d\tau)d\tau\,, \tag{3}$$

where dz/dt is the total velocity in the vertical direction at contact point L_1. In what follows, the equations of motion of the coupled system are derived by employing a Lagrangian formulation and the final results are listed below.

As shown in Fig. 1, two contact forces develop, namely one between the moving mass M and the upper flange of the beam representing the bridge deck $(f_{c,M})$ and a second one at the point of contact of the TMD with the beam's lower flange $(f_{c,m})$. In the former case, the equilibrium equation is

$$M(d^2w_T/dt^2) = Mg - f_{c,M}\,, \tag{4}$$

where $w_T(x = vt, t) = w(x,t) + r(x)$ is the total transverse displacement of the beam that includes the contact surface roughness $r(x)$. The acceleration term in Eq. (4) is computed by the chain rule, yielding the contact force as equal to

$$f_{c,M} = M\left(g - \left(\frac{\partial^2 w}{\partial t^2} + 2v\frac{\partial^2 w}{\partial x \partial t} + v^2\left(\frac{\partial^2 w}{\partial x^2} + \frac{\partial^2 r}{\partial x^2}\right)\right)\right). \tag{5}$$

The total vertical displacement of the TMD's mass m is $w_T(L_1 t) = w(L_1 t) + u_r(t)$, resulting in the following equation of motion:

$$m\ddot{w}_T\left(L_1 t\right) + c\dot{u}_r(t) + ku_r(t) = 0\,. \tag{6}$$

Note that c, k are the TMD's damping element and spring constant. By separating terms,

$$f_{c,m} = c\dot{u}_r(t) + ku_r(t) = -m\left(\ddot{u}_r\left(t\right) + \ddot{w}\left(L_1, t\right)\right). \tag{7}$$

Substituting in the work statement yields a time integral that is easily evaluated by discretizing the time axis using the trapezoidal rule to integrate Eq. (8) at every time step Δt:

$$W\left(t\right) = \int_0^t f_{c,m}\dot{w}_T d\tau = \sum_{n=1}^{N}\{f_{c,m}(n\Delta t)\dot{w}_T(n\Delta t) - f_{c,m}\left((n-1)\Delta t\dot{w}_T\left((n-1)\Delta t\right)\right\} \cdot \Delta t\,. \tag{8}$$

3 Parametric Studies

Numerical values for TMD optimal design have been evaluated in the past by a number of researchers [3,4,17,18] and are listed in Table 1. The optimization criterion is maximum absorption of vibratory energy away from the beam. This information will then be used to numerically gauge the performance of the suboptimal TMD using Eq. (8). For a fixed TMD mass m, the two mechanical parameters that are variable are the restoring spring k and the viscous dashpot c, which in combination with the mechanical properties of the primary system (the beam) yield optimum frequency f_{OPT} and damping ξ_{OPT} ratios. Specifically, μ is the mass ratio between TMD and beam which has a dominant eigenfrequency ω_S and a damping ratio of ξ_S. This information yields an optimal TMD design with a frequency value of ω_D and a damper value of c_D.

It should be noted that all numerical values for the mechanical parameters of the suboptimal TMD case were derived from earlier experiments conducted by the authors [16]. The particular experimental setup used to this purpose is shown in

Fig. 3, and the computations yielding the mechanical properties from the experimental data [19] are listed in Table 2. Next, Table 3 presents numerical values for the frequency and damping ratios of the four optimal designs that were previously listed in Table 1, along with the sub-optimal design that was used in the experimental study. We observe that all four optimal designs predict nearly the same values for the beam-TMD ratios, except for that of Ref. [17] that gives a much higher value for the damping ratio. What differentiates the sub-optimal SDOF design used in the experiments is the near absence of damping, which is provided only by the material damping in the restoring spring without any extra damping element present.

4 Energy Transfer between Primary and Secondary Systems and Overall TMD Performance

Figures 4–6 plot the energy flow at the point of attachment $x = L_1$ between primary and secondary systems for three values of the heavy moving mass M (20, 30, 40 kg

Table 1. TMD frequency f_{OPT} and damping ratios ξ_{OPT} for optimal design

	$f_{OPT} = \omega_D/\omega_S$	$\xi_{OPT} = c_D/2m_D\omega_D$
Den Hartog (1947)	$\dfrac{1}{1+\mu}$	$\sqrt{\dfrac{3\mu}{8(1+\mu)}}$
Warburton (1982)	$\dfrac{\sqrt{1-\mu/2}}{1+\mu}$	$\sqrt{\dfrac{\mu(1-\mu/4)}{4(1+\mu)(1-\mu/2)}}$
Sadek et al. (1997)	$\dfrac{1-\xi_S\sqrt{\mu/(1+\mu)}}{1+\mu}$	$\dfrac{\xi_S}{1+\mu}+\sqrt{\dfrac{\mu}{1+\mu}}$
Leung & Zhang (2009)	$\sqrt{\dfrac{1-\mu/2}{1+\mu}}+(20.23\sqrt{\mu}-37.94\mu-4.945)\sqrt{\mu}\xi_S$ $+(25.00\sqrt{\mu}-4.829)\sqrt{\mu}\xi_S^2$	$\sqrt{\dfrac{\mu(1-\mu/4)}{4(1+\mu)(1-\mu/2)}}$ $-5.302\xi_S^2\mu$

Table 2. Combined primary-secondary structural system measured mechanical properties

Mass density ρ (tn/m^3)	7.65	Beam length L (m)	5.83
Cross-section area A (m^2)	26×10^{-4}	Moving mass M (tn)	0.027
Elasticity modulus E (GPa)	198.5	Moving mass velocity v (m/s)	0.33
Moment of inertia I (m^4)	450×10^{-8}	TMD location L_1 (m)	2.70
1st mode damping ratio ξ_1	0.0021	TMD mass m (tn)	0.0278
2nd mode damping ratio ξ_2	0.0084	TMD stiffness k (kN/m)	122.0
Beam total mass ρAL (tn)	0.116	TMD damping ratio ξ	0.0075

Table 3. Numerical values for the four optimal TMD designs and the present sub-optimal TMD

References	$f_{OPT} = \omega_D/\omega_S$	$\xi_{OPT} = c_D/2m_D\omega_D$
Den Hartog (1947)	0.807	0.269
Warburton (1982)	0.757	0.227
Sadek et al. (1997)	0.806	0.441
Leung and Zhang (2009)	0.752	0.227
Suboptimal design	1.076	0.008

Fig. 3. Experimental setup showing the simply supported beam with the moving mass driven by a wire and the TMD placed at center span with the metallic guides to ensure vertical motion only.

travelling at three different speeds of v = 30, 40, 50 cm/s, thus traversing the beam in T = 20, 15, 12 s, respectively . The energy transfer is measured in kJ and lasts for the traverse time of the mass plus an additional 5 s of free vibrations. During the initial phase of vibration, i.e., at about 20% of the total time duration T, all three TMD's exhibit the same small amount of energy absorption. Subseqeuntly, both optimal TMD's outperform the sub-optimal TMD, but only for small moving masses and at low velocities. As both these mechancial parameters increase, so does the efficiency of the sub-optimal TMD. In fact, for the heaviest mass of 40 kg, the sub-optimal TMD actually performs just as well as the optimal ones. However, it should be noted that in the case of the suboptimal design, vibratory energy is transferred into the TMD when the slope of the energy is negative (i.e., downwards) and back into the beam when the slope is positive (i.e., upwards), while this slope is always negative for the optimal designs. This phenomenon occurs because the absence of a damper in the sub-optimal TMD design allows it to vibrate locally.

Next, we compare the performance of the three different TMD designs in Fig. 7

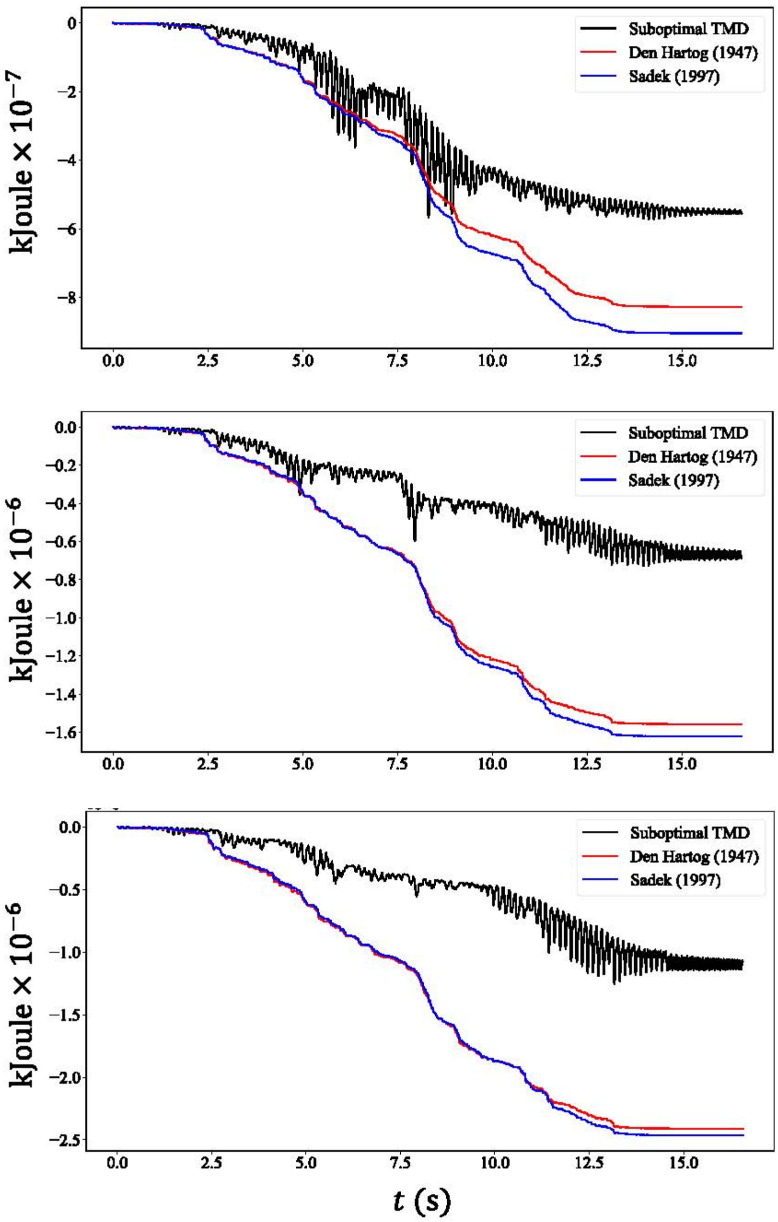

Fig. 4. Energy transfer between the bridge deck and the attached TMD for a travelling speed of $v = 30$ cm/s and masses of $M = 20$, 30, 40 kg (from top to bottom).

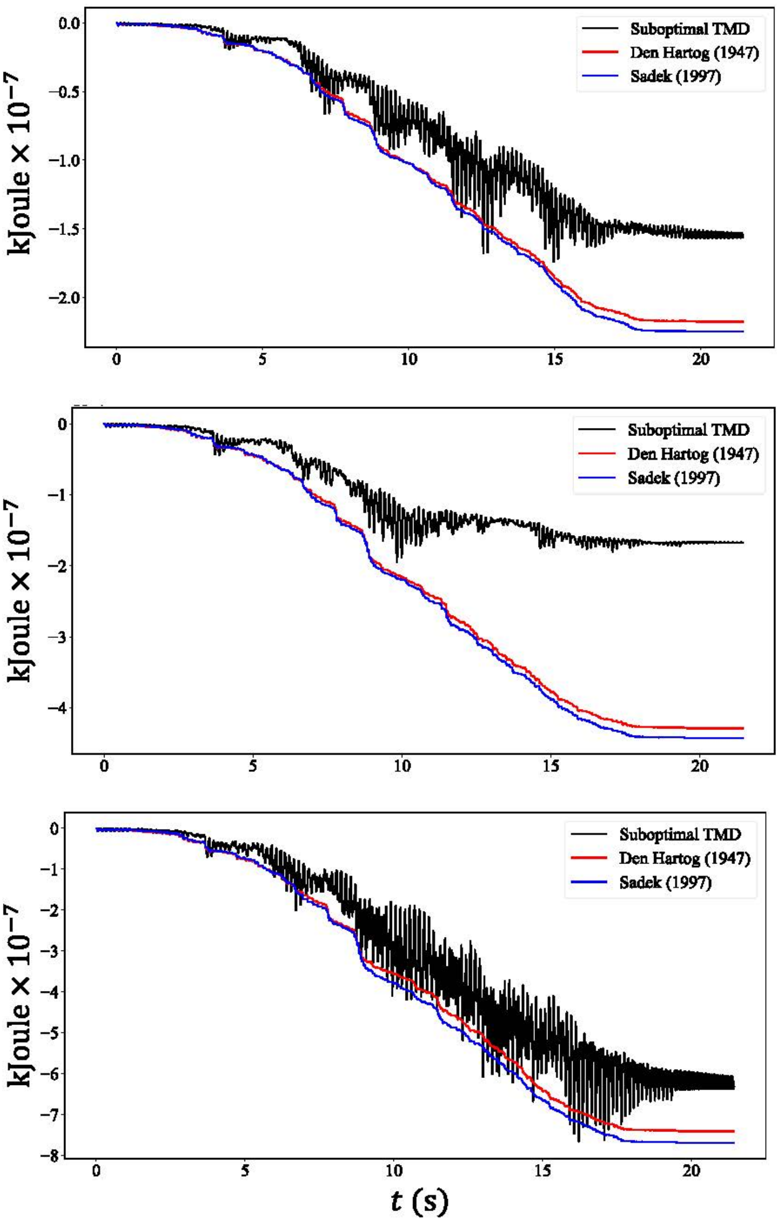

Fig. 5. Energy transfer between the bridge deck and the attached TMD for a travelling speed of $v = 40$ cm/s and masses of $M = 20$, 30, 40 kg (from top to bottom).

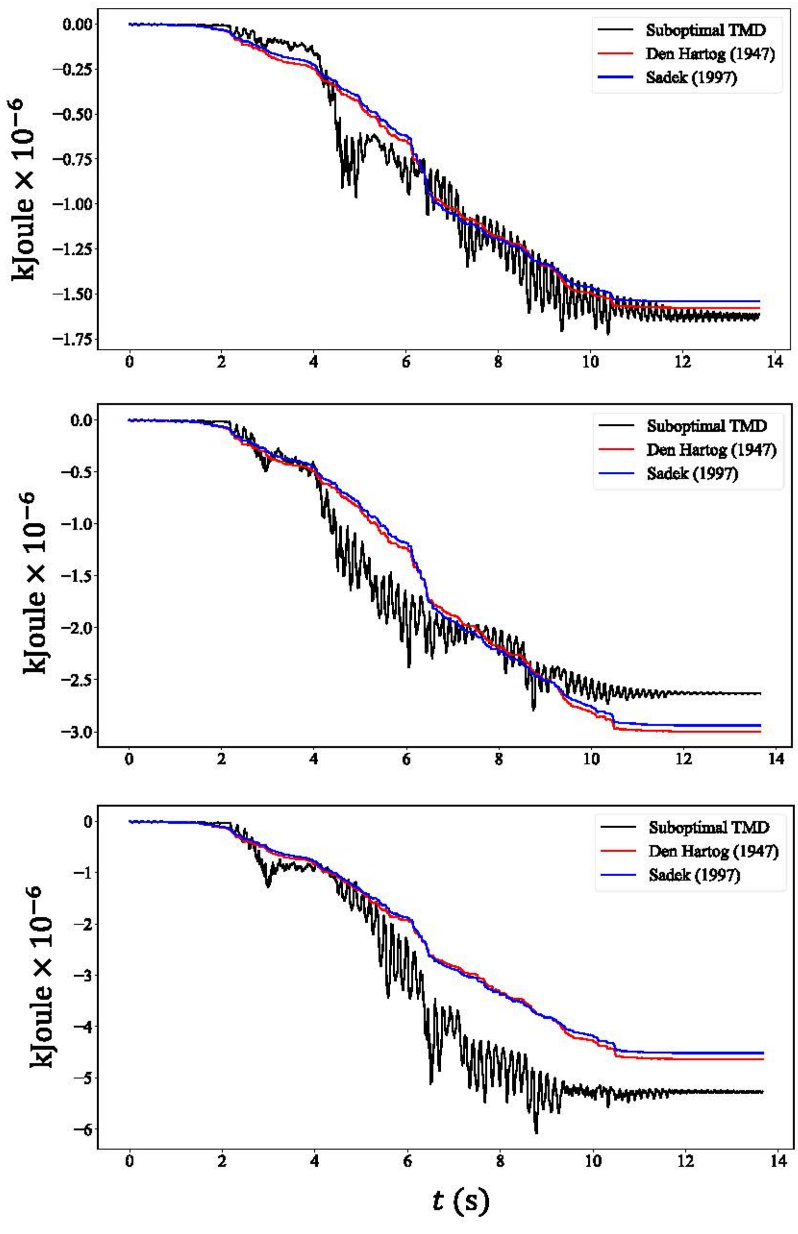

Fig. 6. Energy transfer between the bridge deck and the attached TMD for a travelling speed of $v = 50$ cm/s and masses of $M = 20$, 30, 40 kg (from top to bottom).

in terms of the total accelerations at mid-span location. Note that the acceleration trend over time observed at mid-span for the three TMD may be different at other beam locations, as we have an interplay between the primary-secondary system in the presence of a moving mass, i.e., the interaction problem of Fig. 2. As before, during the first stage of the vibrations, all three TMD's perform similarly, past which the two optimal designs become more effective and their performance is nearly identical. The greatest departure in performance is in the mid-time interval, where the sub-optimal TMD allows for a beam response of ± 0.40 m/s^2, which is double that of the optimal TMD's. Note that the maximum beam acceleration allowed by all TMD's is ± 0.50 m/s^2, recorded in the early stage of the moving mass traverse. In terms of the power spectral density (PSD) of the total accelerations, the optimal TMD's operated around the second eigenfrequency of the beam, while the sub-optimal TMD also allows for vibrations in the range of the first eigenfrequency of the beam.

Finally, Fig. 8 plots the bridge accelerations at mid-span in the presence versus the absence of a sub-optimal TMD, and for the heavy mass of 40 kg travelling at the high velocity of 50 m/s. In general, this TMD is most effective in the free vibration regime following the passage of the moving mass. However, there two time intervals, on in the early and one in the middle time range, where energy is transferred from the TMD to the beam, resulting higher accelerations than would otherwise be recorded in the absence of a TMD.

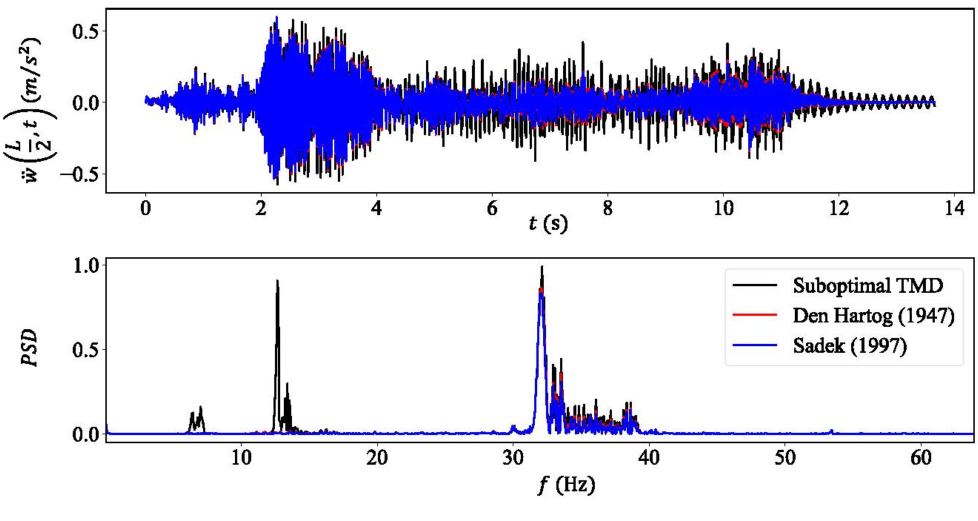

Fig. 7. Bridge total acceleration (top) and the total acceleration power spectral density (PSD) (bottom) at mid-span for a moving mass of $m = 40$ kg moving with velocity $v = 0.50$ cm/s plotted for the suboptimal and two optimal TMD designs.

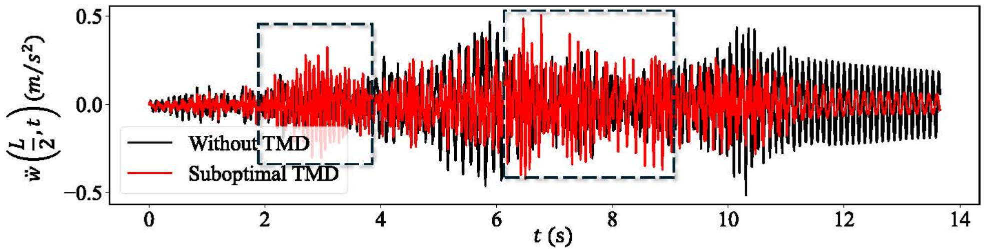

Fig. 8. Bridge total acceleration at mid-span for a moving mass of $m = 40$ kg moving with velocity $v = 0.50$ cm/s. Note: The square boxes indicate the time intervals for which the response of the bridge deck is larger in the presence of the sub-optimal TMD versus in its absence.

In sum, by comparing Figs. 4–6, we observe that the energy absorption time history of the two optimal TMD is consistent and increases continuously with time, while that of the sub optimal TMD is not. This implies that there is a rather pronounced, back and forth, energy transfer between the beam and the suboptimal TMD, resulting in regions where the beam accelerations may be amplified or de-amplified. This is why when comparing Fig. 6c with Fig. 8, we observe see that the suboptimal TMD absorbs more vibratory energy than the other TMD configurations, but over certain time intervals for the case of the large mass moving at high speeds.

5 Conclusions

The use of TMD's to ameliorate the vibratory response of structures under dynamic loads is widespread, as these passive damping devices are easy to place and require virtually no maintenance. Over time, optimal TMD's have been devised that offer a maximum of vibration absorption, but only at a specific frequency range. In this work, we examine the performance of a sub-optimal TMD, namely a SDOF system that comprises a mass attached by a spring to the primary structure, which is a bridge modelled as a simply supported beam. A series of experiments were conducted for the aforementioned setup, where the forcing function was a heavy moving mass, and confirmed the beneficial effect of the TMD. However, the absence of a dedicated damping element causes a two-way energy transfer from the beam to the TMD, combined with the energy imparted to the beam by the travelling mass. This causes the beam's transverse acceleration to be greater compared to the case of no TMD over certain time intervals. In closing, the suboptimal TMD is a simple and economic solution with respect to an optimally designed TMD that includes dampers attached to its mass-stiffness configuration.

Acknowledgement

The first author (G.I.D.) acknowledges the Hellenic Foundation for Research and Innovation (HFRI) for Ph.D. Fellowship No. 6522 under the third call for Ph.D. fellowships. The second author (G.D.M.) acknowledges a Mercator fellowship made available by the German Research Foundation (DFG) project SM 281/20-1 entitled 'Resilient Infrastructure Based on Cognitive Buildings', Kay Smarsly, coordinator, Technical University of Hamburg, Germany. Results presented in this work have been produced using the Aristotle University of Thessaloniki High-Performance Computing Infrastructure.

REFERENCES

[1] J. ORMONDROYE, J.P. DEN HARTOG (1928) The theory of the dynamic vibration absorber. *Transactions of the American Society of Mechanical Engineers* **50**(7) 9-22.

[2] T.T. SOONG, G.F. DARGUSH (1997) "Passive Energy Dissipation Systems in Civil Engineering". John Wiley & Sons, Chichester, UK.

[3] J.P. DEN HARTOG (1947) "Mechanical Vibrations", Third Edition. McGraw-Hill, New York.

[4] G.B. WARBURTON (1982) Optimum absorber parameters for various combinations of response and excitation parameters. *Earthquake Engineering Structural Dynamics* **10** 381-401.

[5] S.H. CRANDALL, W.D. MARK (1963) "Random Vibration in Mechanical Systems". Academic Press, New York.

[6] D.J. INMAN (2013) "Engineering Vibrations", Fourth edition. Pearson Education, London.

[7] R.K. KUMAR, A. KUMAR (2023) Vibration suppression and stability analysis of a beam at large amplitude excitation using a two-degree-of-freedom nonlinear energy sink. *Acta Mechanica* **235** 971-990.

[8] F. YANG, R. SEDAGHATI, E. ESMAILZADEH (2022) Vibration suppression of structures using tuned mass damper technology: A state-of-the-art review. *Journal of Vibration and Control* **28**(7-8) 812-836.

[9] S.H.H. LAVASSANI, D.P.N. KONTONI, H. ALIZADEH, V. GHAREHBAGHI (2023) Passive control of ultra-span twin-box girder suspension bridges under vortex-induced vibration using tuned mass dampers: A sensitivity analysis. *Buildings* **13** 1279.

[10] S.R. CHEN, J. WU (2008) Performance enhancement of bridge infrastructure systems: Long-span bridges, moving trucks and wind with tuned mass dampers. *Engineering Structures* **30** 3316-3324.

[11] C. ADAM, S. DI LORENZO, G. FAILLA, A. PIRROTTA (2017) On the moving load problem in beam structures equipped with tuned mass dampers. *Meccanica* **52** 3101-3115.

[12] K. VAN NIMMEN, P. VERBEKE, G. LOMBAERT, G. DE ROECK, P. VAN DEN BROECK (2016) Numerical and experimental evaluation of the dynamic performance of a footbridge with tuned mass dampers. *ASCE Journal of Bridge Engineering* **21**(8) C4016001.

[13] H. HOMAEI, E.G. DIMITRAKOPOULOS, A. BAKHSHI (2023) Vehicle-bridge interaction and the tuned-mass damper effect on bridges during vertical earthquake excitation. *Acta Mechanica* **235** 1379–1394.

[14] G.D. MANOLIS, A. ATHANATOPOULOU-KYRIAKOU, K.D. DRAGOS, A. ARABATZIS, A. LAVDAS, C.Z. KARAKOSTAS (2014) Identification of Pedestrian Bridge Dynamic Response through Field Measurements and Numerical Modeling: Case Studies. *Journal of Theoretical and Applied Mechanics of the Bulgarian Academy of Sciences, General Mechanics Series* **44**(2) 3-24.

[15] G.I. DADOULIS, G.D. MANOLIS (2023) Dynamic Response of a Damaged Bridge Span Traversed by a Heavy Point Mass. *Journal of Sound and Vibration* **551** 117613.

[16] G.D. MANOLIS, G.I. DADOULIS (2024) Passive Control in a Continuous Beam under a Travelling Heavy Mass: Dynamic Response and Experimental Verification. *Sensors* **24**(2) 573.

[17] F. SADEK, B. MOHRAZ, A.W. TAYLOR, R.M. CHUNG (1997) A method of estimating the parameters of tuned mass dampers for seismic applications. *Earthquake Engineering Structural Dynamics* **26** 617-635.

[18] A.Y.T. LEUNG, H. ZHANG (2009) Particle swarm optimization of tuned mass dampers. *Engineering Structures* **31**(3) 715-728.

[19] G.I. DADOULIS, G.D. MANOLIS (2024) A Comparative Study on the Effectiveness of a Moving versus a Stationary Passive Damper in Beam Vibration Mitigation. *Acta Mechanica* **235** 6403-6412.